

Fig. 3. Relationship between dissipation power and maximum counting frequency.

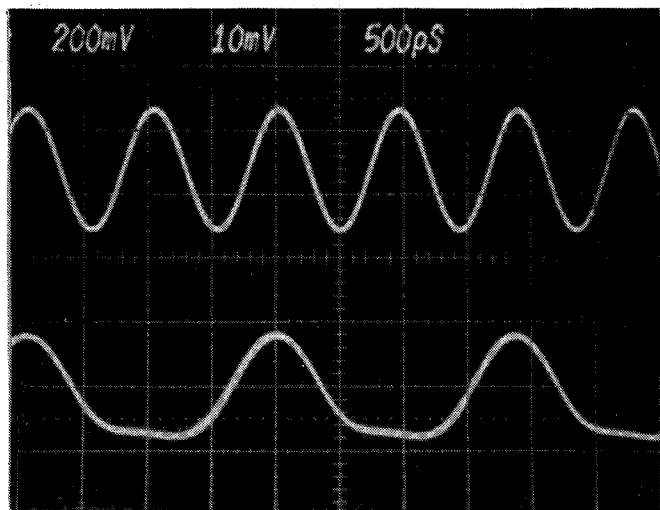


Fig. 4. Input/output waveforms of the developed divider.

gate width) at 1.1-GHz input frequency, which were observed by a  $50\Omega$  system connected to the drain of the output buffer circuit.

#### IV. CONCLUSION

GaAs frequency dividers for application to gigahertz-band equipment have been developed with E/D DCFL circuits. The relationship between maximum counting frequency and threshold voltage, which are the critical design parameters of the divider circuit, have been shown in detail. The measured performance was as follows: maximum counting frequency is 1.1 GHz with low dissipation power of 17 mW, and the values of dissipation-power-divided-by-maximum-counting-frequency are as small as 1.6–16 pJ.

#### ACKNOWLEDGMENT

The authors wish to thank Dr. T. Suzuki, Dr. H. Ariyoshi, Dr. M. Ohmori, Dr. S. Seki, Dr. K. Ayaki, and Dr. H. Kato for useful discussions and continuous encouragement through this work.

#### REFERENCES

- [1] R. C. Eden, B. M. Welch, R. Zucca, and S. I. Long, "The prospects for ultra-high-speed VLSI GaAs digital logic," *IEEE Trans. Solid-State Circuits*, vol. SC-14, pp. 221–239, Apr. 1979.
- [2] F. Katano, T. Furutsuka, A. Higashisaka, and K. Kurumada, "A study on fabrication of normally off GaAs MESFET with short inter-gate-source and inter-gate-drain length," (in Japanese) in *Proc. 1981 Nat. Conv. Semiconductor and Materials, Inst. Electron. Commun. Eng. Japan*, p. 117, Oct. 1981.
- [3] K. Lchovc and R. Zuleeg, "Voltage-current characteristics of GaAs J-FET's in the hot electron range," *Solid-State-Electron.*, vol. 13, pp. 1415–1426, 1970.
- [4] M. Ino, K. Kurumada, and M. Ohmori, "Performance forecast on GaAs static memories," (in Japanese) in *Proc. 1981 Nat. Conv. Semiconductor and Materials, Inst. Electron. Commun. Eng. Japan*, p. 126, Oct. 1981.
- [5] T. Furutsuka, T. Tsuji, F. Katano, A. Higashisaka, and K. Kurumada, "An ion-implanted E/D GaAs IC technology," *Electron. Lett.*, vol. 17, no. 25, pp. 944–945, Dec. 1981.
- [6] T. Mizutani, N. Kato, S. Ishida, K. Osafune, and M. Ohmori, "GaAs gigabit logic circuits using normally off MESFET's," *Electron. Lett.*, vol. 16, no. 9, pp. 315–316, Apr. 1980.
- [7] R. L. Van Tuyl, C. A. Liechti, R. E. Lee, and E. Gowen, "GaAs MESFET logic with 4-GHz clock rate," *IEEE J. Solid-State Circuits*, vol. SC-12, no. 5, Oct. 1977.
- [8] M. Cathelin, G. Durand, M. Gavant, and M. Rocchi, "5-GHz binary frequency division on GaAs," *Electron. Lett.*, vol. 16, no. 14, pp. 535–536, July 1980.
- [9] F. Katano, T. Furutsuka, and A. Higashisaka, "High-speed normally off GaAs MESFET integrated circuit," *Electron. Lett.*, vol. 17, no. 6, pp. 236–237, Mar. 1981.
- [10] M. Gloanec, J. Jarry, and G. Nuzillat, "GaAs digital integrated circuits for very high-speed frequency division," *Electron. Lett.*, vol. 17, no. 20, pp. 763–765, Oct. 1981.

#### Losses in Coplanar Waveguides

A. GOPINATH

**Abstract**—Conductor losses in coplanar waveguides have been calculated using a quasi-static Green's function approach. These calculations and others on dielectric and radiation losses are used to compute the quality factor of half-wavelength resonators, and comparison with measurements show good agreement.

#### I. INTRODUCTION

The coplanar waveguide (CPW) is a planar guiding structure (Fig. 1) sometimes suggested as an alternative to microstrip lines [1], [2] in both hybrid and monolithic circuits. Losses in these guides have been investigated by several authors [3]–[6] over a limited range of parameters.

The present paper calculates the conductor losses in a coplanar waveguide, using a quasi-static approach, and provides a comprehensive set of results. The quality factors of half-wavelength resonators including radiation losses are calculated and the results are compared with experimental measurements on resonators on substrates with a relative dielectric constant  $\epsilon_r$  of 13.0.

#### II. CALCULATION OF COPLANAR WAVEGUIDE PARAMETERS

The various parameters of the coplanar waveguide are calculated for different strip width to ground plane spacing ratios ( $2a/2b$ ) (see Fig. 1), assuming quasi-static TEM propagation.

Manuscript received September 27, 1981; revised February 23, 1982. This work was sponsored by the Department of the Army. The U.S. Government assumes no responsibility for the information presented.

The author was with M.I.T. Lincoln Laboratory, Lexington, MA. He is now with the Department of Electronics, Chelsea College, University of London, Pulten Place, London SW6 5PR, England.

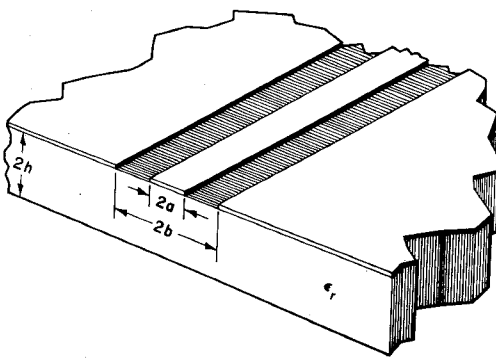
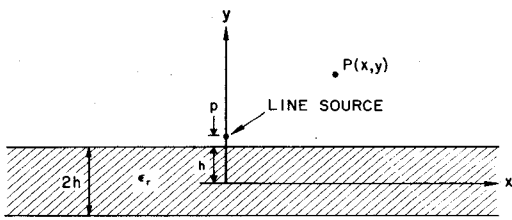


Fig. 1. Geometry of coplanar waveguide.

Fig. 2. Observation point  $P$  and line source over substrate, used in derivation of the quasi-static Green's function.

The Green's function for a line charge distance  $p$  from the surface of dielectric slab of thickness  $2h$  is derived using the method of images [7]. For the observation point  $P$  at  $(x, y)$ , in the same air space as the line charge at  $(0, h + p)$  of  $q$  C/m (see Fig. 2), the potential at  $P$  is given by

$$V(x, y) = -\frac{q}{4\pi\epsilon_0} \log \frac{(y - h - p)^2 + x^2}{R^2} - \frac{Kq}{4\pi\epsilon_0} \cdot \log \frac{(y - h + p)^2 + x^2}{R^2} + \frac{(1 - K^2)q}{4\pi\epsilon_0} \cdot \sum_{n=1}^{\infty} K^{2n-1} \log \frac{(y + (4n-1)h + p)^2 + x^2}{R^2}$$

where

$$K = \frac{\epsilon_0 - \epsilon_1}{\epsilon_0 + \epsilon_1}$$

$$R^2 = (x - x_p)^2 + (y - y_p)^2$$

$\epsilon_1 = \epsilon_r \epsilon_0$  the substrate dielectric constant

$(x_p, y_p)$  = coordinates of the point with constant reference potential. (1)

The quantity  $R$  is the distance from the observation point to the reference potential point. In the present instance, this reference point was chosen to be the center of the conducting strip.

The ground planes on either side of the strip are assumed to be of finite width over the infinitely wide substrate of finite thickness  $2h$ . The strip and ground planes are subdivided into substrips and the charge distribution over each substrip is assumed to be uniform, but unknown in magnitude. The problem is solved by the usual matrix equation derived from the equation

$$V = \int \sigma_l G dl \quad (2)$$

where  $V$  is the potential on the strip and ground planes, and  $\sigma_l$  is the unknown charge distribution over the substrips. The strip and ground-plane potentials are assumed to be unknown and set at +1 and 0 V, respectively.

It is necessary, however, to impose the condition that the total charge on the strip is equal and opposite to the sum of the total charges on the ground planes. This condition is imposed by using the null matrix technique discussed in detail elsewhere [8]. In brief, this condition gives rise to a rectangular matrix equation, the null space of which represents a new basis-function set, which satisfies this equation and can be used as trial functions in (2).

The charge patterns are obtained without and with the substrate, and from these the capacitances  $C_o$  and  $C_d$  are obtained and hence the impedance, velocity factor, and effective dielectric constant  $\epsilon_{\text{eff}} \epsilon_0$  are calculated.

### III. CONDUCTOR AND DIELECTRIC LOSS CONSTANTS

The charge pattern without the dielectric substrate corresponds to the longitudinal current distribution pattern and from this the conductor loss factor  $\alpha_c$  is evaluated from

$$\alpha_c = \frac{R_s}{2Z_0 I^2} \int_{-a}^{+a} J_s^2 dx + 2 \int_b^{b_{\max}} J_{gp}^2 dx \text{ Np/m} \quad (3)$$

where  $J_s$  is the strip longitudinal current linear density,  $J_{gp}$  is the ground-plane current linear density,  $Z_0$  is the characteristic impedance of the CPW,  $I$  is the total strip or ground-plane current, and  $R_s$  is the metal surface resistivity in ohms.

Since the substrate loss tangent is generally small, the plane-wave approach may be used to evaluate the dielectric loss constant  $\alpha_d$ . Thus

$$\alpha_d = \frac{q\epsilon_r \tan \delta}{\epsilon_{\text{eff}} \lambda_g} \text{ Np/m} \quad (4)$$

where  $\epsilon_r$  is the substrate relative dielectric constant,  $\epsilon_{\text{eff}}$  is the relative effective dielectric constant of the guide,  $\lambda_g$  is the guide wavelength, and  $q$  is the guide filling factor,  $(\epsilon_{\text{eff}} - 1)/(\epsilon_r - 1)$ .

### IV. QUALITY FACTORS OF HALF-WAVELENGTH RESONATORS

The stored energy  $U$  in a  $\lambda_g/2$  resonator with a voltage distribution  $V \sin \beta_g z$  is given by

$$U = \frac{V^2}{8Z_0 f}. \quad (5)$$

The losses in the resonator arise from conductor dissipation, dielectric loss dissipation, and radiation. The conductor and dielectric losses are given by

$$W_c = \frac{1}{4} \frac{V^2}{Z_0} \lambda_g (\alpha_c + \alpha_d) \quad (6)$$

and the circuit quality factor  $Q_c$  is given by

$$Q_c = \frac{2\pi f U}{W_c} = \frac{\pi}{\lambda_g (\alpha_c + \alpha_d)}. \quad (7)$$

The radiation quality factor is given by

$$Q_r = \frac{2\pi f U}{W_r} \quad (8)$$

where  $W_r$  is the radiated power, estimated below. The total

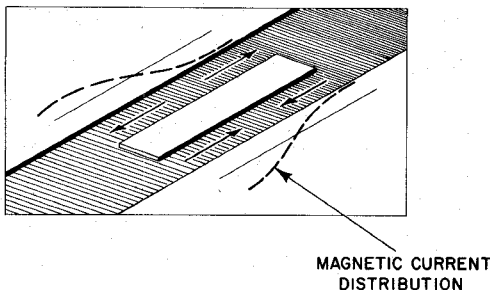


Fig. 3. Distribution of magnetic currents in the strip to ground-plane gaps for radiation calculations.

quality factor  $Q_t$  is given by

$$\frac{1}{Q_t} = \frac{1}{Q_r} + \frac{1}{Q_c} \quad (9)$$

#### V. RADIATION LOSS FROM A HALF-WAVELENGTH RESONATOR

Radiation losses may only be estimated for finite lengths of line. The exact calculation of radiation loss from a half-wavelength CPW resonator has not been performed, and therefore an approximate method was used.

The two slots on either side of the  $\lambda_g/2$  resonator between the strip and the ground planes are assumed to have magnetic currents that radiate into the air half-space and the half-space comprising substrate and the lower air space, if any. When the substrate fills this half-space, then the calculation is greatly simplified, and the radiation from the magnetic currents, whose distributions are known, may be readily estimated into each half-space. However, since the guide wavelength is longer than the dielectric free-space wavelength, the radiation in this half-space is very efficient, and in fact such calculation for the finite thickness substrate resonators overestimate the radiated power.

When the substrate is of finite thickness, the calculation of radiated power in this half-space is difficult. An approximation adopted here assumes that the half-space is filled with dielectric whose relative permittivity is  $\epsilon_{\text{eff}}$ . The combination of this with the other half-space filled with air provide an estimate of radiated power which may be acceptable.

The coplanar waveguide  $\lambda_g/2$  resonators may be either open circuit or short circuit at their ends. Since the former case has smaller radiation losses and therefore higher radiation quality factors, it is calculated here; the latter case follows on similar lines. Fig. 3 shows the distribution of magnetic currents in the slot regions and for the open-circuit  $\lambda_g/2$  resonator the currents have a  $\pm \sin \beta_g z$  variation. The antiphase excitation and the change in direction of the current along the element reduces the radiated power.

For a vertical conducting plane with an open circuit CPW  $\lambda_g/2$  resonator with two slots, each of width given by  $g$  (equal to  $b - a$ ), and spaced  $d$  (equal to  $b + a$ ) apart, the total  $E$ -field in any of the half-spaces is given by

$$E_T = \bar{a}_\phi \frac{k_m^2 g E_m}{\pi r} \frac{\sin 2\theta \cos \left( \frac{k_m l}{2} \cos \theta \right)}{\left( \beta_g^2 - k_m^2 \cos^2 \theta \right)} \cdot \sin \left( \frac{k_m d}{2} \sin \theta \cos \phi \right) e^{-j k_m r} \quad (10)$$

where the voltage across the guide  $V = g E_m$ , and  $k_m$  is the

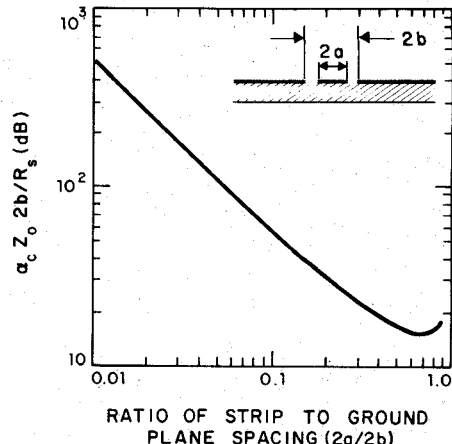


Fig. 4. Normalized conductor loss constant  $\alpha_c 2b Z_0 / R_s$  plotted against the strip width to ground-plane spacing ratio  $2a/2b$ .

propagation constant of the medium, either air space or effective dielectric constant space. The radiated power in each half-space is given by

$$W_{a, \text{def}} = \frac{1}{2\eta_{a, \text{def}}} \int_0^\pi \int_0^\pi (E_T)^2 r^2 \sin \phi d\theta d\phi \quad (11)$$

where  $\eta_{a, \text{def}}$  is the impedance of the appropriate half-space. Note that  $\eta_{\text{def}}$  is the impedance of the half-space of dielectric constant  $\epsilon_{\text{eff}}$ . The integrations are performed numerically for each half-space in turn and the total radiated power is equal to their sum.

#### VI. COMPUTATION OF LOSSES AND QUALITY FACTORS

A computer program has been written to calculate the impedance, wave velocity, and effective dielectric constant of coplanar waveguides for finite substrate thickness  $2h$ , and finite metallization thickness  $2t$ . The substrips are assumed to lie at the top and bottom of the strip and each ground plane, and the charge on each of these is obtained from the solution of the matrix equation. To increase the accuracy of the computation, the substrips are subdivided to be narrow in width close to the edges of the strip and inner edge of the ground planes and wider elsewhere. The conductivity of the upper and lower metallization layers corresponding to the respective substrips may also be specified as being different. The corresponding conductor loss constant and the dielectric loss constant are calculated based on these factors. At the specified frequencies, the circuit, radiation, and total quality factors of  $\lambda_g/2$  resonators are also calculated. In these calculations  $b_{\text{max}}$  was equal to 20b.

A recent paper [9] has questioned the validity of using (3) in such loss calculations. The present calculations have been performed using a finite conductivity, finite (i.e., constant) basis functions, and uses the "thick strip" approach, all of which lead to a bounded solution. Increasing the substrip numbers from 24 to 72 metalized region has also resulted in the normalized conductor loss constant converging to such bounded solutions. It would therefore appear that comments from the above paper are not applicable to the present calculations.

#### VII. COMPUTATIONAL RESULTS AND COMPARISON WITH EXPERIMENTS

As there is adequate information in the literature [1]–[6] regarding the variation of  $Z_0$  and  $\epsilon_{\text{eff}}$  with  $a/b$  for coplanar waveguides, these results are not included here. The normalized

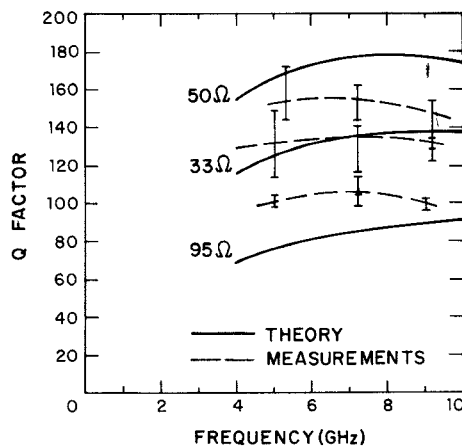


Fig. 5. Half-wavelength resonator quality factor plotted against frequency for resonators on substrates with  $\epsilon_r = 13.0$ , thickness 0.635 mm, and ground-plane spacing  $2b = 1.2$  mm.

conductor loss curve is given in Fig. 4, and from this, conductor losses for any ground-plane spacing may be obtained.

Quality factors of  $\lambda_g/2$  resonators were calculated for  $\epsilon_r = 13.0$  substrate, 0.635 mm thick, and ground plane spacing of 1.2 mm. Experimental measurements were performed on open-circuit resonators on Trans Tech D-13 substrates 0.635 mm thick for this ground-plane spacing of 1.2 mm. To extract the unloaded  $Q$ , the loss in the feed line was also taken into account in the usual manner. The comparison between theory and experiment is shown in Fig. 5, where the best agreement is for the 33- $\Omega$  resonators. Measurements of the  $Q$ -factors of resonators with the wider ground-plane spacing of 1.75 mm (not shown here) were lower by about 20 percent than predicted by the theory. The conductor-loss constants calculated here show reasonable agreement with other measurements [5] and predictions [6].

### VIII. CONCLUSIONS

The losses in coplanar waveguides have been calculated and a normalized conductor loss curve is provided. The quality factors of half-wavelength resonators including radiation effects have been computed and show agreement with measured values.

### REFERENCES

- [1] C. P. Wen, "Coplanar waveguides: A surface strip transmission line suitable for nonreciprocal gyromagnetic device application," *IEEE Trans. Microwave Theory Tech.*, vol. MTT-17, pp. 1087-1090, 1969.
- [2] M. E. Davies, E. W. Williams, and A. C. Celestine, "Finite boundary corrections to coplanar waveguide analysis," *IEEE Trans. Microwave Theory Tech.*, vol. MTT-23, pp. 795-802, 1975.
- [3] B. E. Spielman, "Computer-aided analysis of dissipation losses in isolated and coupled transmission lines for microwave and millimeter wave integrated circuit applications," Naval Research Laboratory, Washington, DC, NRL Rep 8009, 1979.
- [4] J. B. Davies and D. Mirshekhar-Syakhal, "Spectral domain solution of arbitrary coplanar transmission line with multilayer substrates," *IEEE Trans. Microwave Theory Tech.*, vol. MTT-25, pp. 143-146, 1977.
- [5] J. A. Higgins, A. Gupta, G. Robinson, and D. R. Ch'en, "Microwave GaAs FET monolithic circuits," in *Int. Solid State Circuits Conf. Dig.*, 1979, pp. 20-21.
- [6] K. C. Gupta, R. Garg, and I. J. Bahl, *Microstrip Lines and Slot Lines*. Dedham, MA: Artech House, 1979.
- [7] P. Silvester, "TEM properties of microstrip transmission lines," in *Proc. Inst. Elec. Eng.*, vol. 115, 1968, pp. 42-49.
- [8] A. Gopinath and P. Silvester, "Calculation of inductance of finite length strips and its variation with frequency," *IEEE Trans. Microwave Theory Tech.*, vol. MTT-21, pp. 380-386, 1973.
- [9] R. Pregla, "Determination of conductor losses in planar waveguide structures," *IEEE Trans. Microwave Theory Tech.*, vol. MTT-28, pp. 433-434, 1980.

## Transmission Loss of Thick-Film Microstriplines

SADAYUKI NISHIKI AND SHUOMI YUKI

**Abstract** — Thick-film microstripline transmission loss is measured and discussed, and an empirical formula for thick-film microstripline transmission loss is obtained. It is found that the transmission loss of copper thick film is nearly equal to that of thin film for frequencies up to 10 GHz.

### I. INTRODUCTION

Thick-film technology is widely applied to mass-produced radio equipment such as citizen-band transceivers, televisions, and radio tuners with good volume production yield. However, in the microwave region, thin-film technology is generally used to fabricate hybrid integrated circuits, because 1) there have been few hybrid integrated circuits to be mass produced in the microwave region, 2) thick-film microstripline has possessed higher transmission loss than that of thin film, and 3) printing and baking methods for making thick-film microstripline have made it difficult to form fine patterns.

However, various conductive thick-film materials have been developed. The composition of thick-film binders has undergone various improvements, and the sheet resistance has been reduced. Ramy has reported that thick film can be utilized like thin film [1].

In our experiment, the microstripline transmission losses of various thick-film materials were measured. As a result of these measurements, an empirical formula for thick-film transmission loss was obtained. In this paper, we would like to discuss our findings concerning thick-film transmission loss.

### II. THICK-FILM MICROSTRIPLINE

Table I gives the thick-film materials used, and their dc sheet resistance after baking.

The thick-film microstripline was applied with a No. 200 mesh<sup>1</sup> mask onto the alumina ceramic substrate. Fig. 1 shows the thick-film microstripline pattern obtained. Its corners were mitered, as shown in Fig. 1. Its total length was 26 cm and its characteristic impedance was 50  $\Omega$  [2]. The same thick film as that for the microstripline was also used for the ground electrode on the opposite side of the substrate. Also, in order to make a comparison with the thick film, an identical thin-film microstripline was produced. A 500- $\text{\AA}$  thick layer of chromium was evaporated in a vacuum on the alumina substrate, which was followed by a 5000- $\text{\AA}$  thick layer of gold. It was then electro-plated with 5  $\mu\text{m}$  of gold.

Table II shows the specifications for the alumina ceramic substrate used with the thick and thin films. The thickness of these substrates is 0.635 mm.

The surface roughnesses of the substrate are shown in Fig. 2. The substrate of the thin film is almost flat, while that of the thick film is of a surface roughness of about 2  $\mu\text{m}$  peak to peak. Fig. 3 is a comparison of the profiles of the thick- and thin-film microstriplines measured with a surface tester after baking. The section of the thin film is practically rectangular, while that of the thick film is rounded at the edges, and there is a slight roughness

Manuscript received November 12, 1981; revised February 25, 1982.

The authors are with Yokosuka Electrical Communication Laboratory, Nippon Telegraph and Telephone Public Corp., 1-2356, Take, Yokosuka-shi, Kanagawa-ken, 238-03, Japan.

<sup>1</sup>No. 200 mesh is formed by 200 40  $\mu\text{m}$   $\phi$  running vertically and horizontally within a one inch square space.